Functional mesoporous carbon nanotubes and their integration in situ with metal nanocrystals for enhanced electrochemical performance

Jiang, Hao; Zhao, Ting; Li, Chunzhong; Ma, Jan

2011

Jiang, H., Zhao, T., Li, C., & Ma, J. (2011). Functional mesoporous carbon nanotubes and their integration in situ with metal nanocrystals for enhanced electrochemical performances. Chemical Communications, 47(30), 8590-8592.

https://hdl.handle.net/10356/93904

https://doi.org/10.1039/C1CC12942B

Functional Mesoporous Carbon Nanotubes and Their Integration *in Situ* with Metal Nanocrystals for Enhanced Electrochemical Performances

Hao Jiang,[a, b] Ting Zhao,[c] Chunzhong Li*,[a] and Jan Ma*,[b, c]

Received (in XXX, XXX) Xth XXXXXXXXX 200X, Accepted Xth XXXXXXXXX 200X
DOI: 10.1039/b000000x

Functional mesoporous carbon nanotubes (MCNTs) and their integration *in situ* with Pt nanocrystals (Pt/MCNTs) have been designed and successfully developed via a facile route, which exhibited enhanced performances in energy storage and conversion applications.

One of the great challenges for our society is to provide high-efficient, low-cost and environmentally friendly electrochemical energy conversion and storage devices.[1] It is noteworthy that the performance of these devices depends intimately on the properties of the materials. Carbon materials, especially one-dimensional carbons, such as carbon fibers and carbon nanotubes (CNTs), have attracted great interest due to their high surface area and short diffusion path to ions and excitons, making them ideal candidates for electrode materials and catalyst supports.[2] However, carbon fibers suffer from poor mechanical strength as they contain a variety of structural defects.[3] CNTs, on the other hand, have been well accepted that they have superior electrical properties with unique tubular structures, which favor fast ion and electron transportation.[4] However, the entanglement problem of CNTs results in poor efficiency in facilitating fast ionic transportation.[5] Furthermore, considering the difficulty in purification and high cost of CNTs, it is desirable to develop a simple low-cost route to synthesize novel one dimensional carbon materials with excellent electrochemical properties.

On the other hand, it is well known that the performance of heterogeneous catalysts is highly affected by their support materials.[6] As mentioned earlier, CNTs have also been considered as an attractive candidate for support materials, especially with the integration of metal nanocrystals for fuel cell catalysts. However, the effective attachment of metal nanocrystals, and also their uniform dispersion onto CNTs, remains a great challenge because of the inertness of the CNTs walls.[7] Until now, a tedious pretreatment procedure is still needed to modify CNTs walls and complex equipment is required to achieve high dispersion of the metal nanocrystals on CNTs.[8] It is, nevertheless, noted that the well-distribution of metal nanocrystals on the external walls is highly desired to establish the better contact between catalysts and reactants. Therefore, extensive efforts have been put into the research of an efficient and facile method to realize uniform distribution of metal nanocrystals on the outside surface of CNTs.

One-dimensional mesoporous carbon nanotubes are therefore reckoned to be the goal for high-performance electrochemical applications, which may have huge potentials to overcome the shortcoming of CNTs. Unfortunately, to date, there have been limited reports on the development of mesoporous carbon nanotubes. In the present work, functional mesoporous carbon nanotubes (MCNTs) and their integration in situ with Pt nanocrystals (Pt/MCNTs) have been designed and successfully developed by a facile route, demonstrating enhanced electrochemical properties.

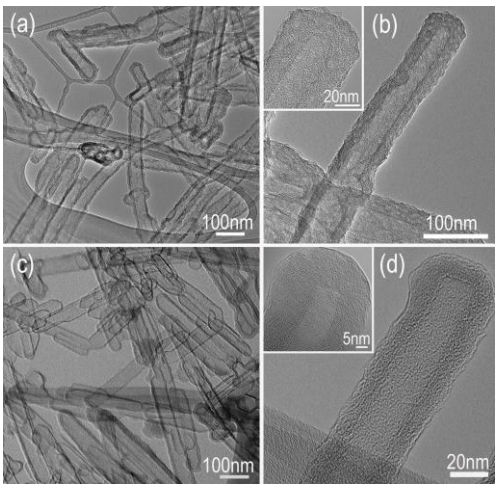

Fig. 1 (a, c) Low magnification and (b, d) high magnification TEM images of MCNTs and CCNTs, respectively.

The synthesis strategy for MCNTs and Pt/MCNTs has been illustrated in Figure S1 (see ESI). Here, ZnO nanorods acts as a template. Dopamine and P123 were chosen as carbon sources and the generation of mesoposous structures according to our pervious work.[9] Figure 1a shows the low magnification TEM image of the as-synthesized MCNTs. It can be seen that the products are remarkably uniform and clean, no other carbon allotropes like graphite or amorphous clustered materials is observed. The average thickness of the carbon layer was estimated to be ~ 17.2 nm. Figure 1b reveals the mesoporous carbon feature with the pore size of ~ 3.9 nm. No residual ZnO crystal lattice can be observed, showing that highly pure carbon materials are produced using the present strategy, which was further confirmed by EDS results (see ESI). For comparison, closed carbon nanotubes (labeled as CCNTs) have also been synthesized by the same procedure but without the addition of P123, as shown in Figure 1c. The thickness of carbon layer was estimated to be about 8.5 nm. No obvious mesopores was observed from high magnification TEM image (Figure 1d). Furthermore, the MCNTs also show a higher specific surface area of 224 m^2 g^{-1} with uniform pore size distribution of 3.9 nm (see Figure S2, ESI).

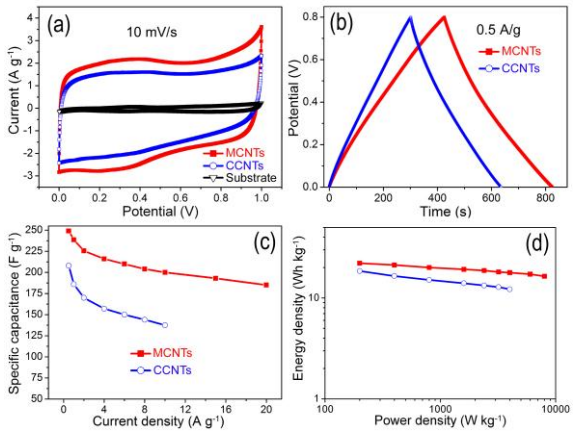

Fig. 2 Electrochemical performance of MCNTs and CCNTs in 1 M H_2SO_4: (a) CV curves at 10 mV s^{-1}, (b) Galvanostatic charge/discharge curves at 0.5 A g^{-1}, (c) Relationship of the specific capacitance with respect to the charge/discharge specific currents, and (d) Ragone plots.

To examine the capacitive properties of our present MCNTs materials, cycle voltammogram (CV) and galvanostatic charge-discharge (CD) measurements were carried out in 1 M H_2SO_4. Figure 3a shows the CV curves of the present MCNTs, CCNTs and substrate at a scan rate of 10 mV s^{-1}. The CV curve of the substrate indicated that its effect to the results is negligible. Both MCNTs and CCNTs samples present a typical capacitive behavior with a rectangular and symmetric CV curve. It is obvious that MCNTs possess a higher specific capacitance. Even at a scan rate as high as 500 mV s^{-1}, the CV curves (see Figure S4, ESI) still maintain a relatively good rectangular shape, indicating their high-power capacitor behaviors. Furthermore, the materials are also reckoned to possess heteroatom functionalities from the redox peaks observed at the range of 0.2−0.4 V in the CVs curves, which indicate the capacitive response comes from the combination of EDLCs and redox reactions.[10]

Figure 2b shows the charge/discharge curves of both MCNTs and CCNTs materials at a current density of 0.5 A g^{-1}. It can also be seen that the charging curves are symmetric to their corresponding discharge counterparts. It is noted that the specific capacitance of the MCNTs can achieve a maximum of 249 F g^{-1}, which is significantly higher than that of the CCNTs (208 F g^{-1}). Even at 20 A g^{-1}, the specific capacitance of MCNTs still remains 185 F g^{-1} (about 75% retention). The relationships between specific capacitance and charge/discharge current density for MCNTs and CCNTs are illustrated in Figure 2c. MCNTs samples have shown a superior rate capability performance than that of the CCNTs samples (137 F g^{-1} at 10 A g^{-1}, 66% retention). It is possible that some micropores in CCNTs do not participate in the formation of the double layer.[11] Such excellent electrochemical properties are better than most of the reported carbon materials, such as single-wall CNTs (180 F g^{-1}),[12] graphene nanosheets (175 F g^{-1} at 10 mV s^{-1}, 210 F g^{-1} for the MCNTs)[13] and self-assembled graphene hydrogel (175 F g^{-1} at 10 mV s^{-1})[14]. In a previous study,[15] it was reported that the specific capacitance of activated carbon with specific surface area as high as 3000 m^2 g^{-1} could reach ~ 300 F g^{-1}. However, at a high current density, the specific capacitance may drop dramatically because of their tortuous pore structure and high microporosity.[16] In our case, the precursor, i.e. polydopamine, containing a high concentration of functional groups, introduces heteroatoms into the carbon materials as result of the incomplete carbonization. The heteroatoms can participate in pseudofaradaic charge-transfer reactions, significantly enhancing the specific capacitance of the as-obtained MCNTs through introducing additional pseudocapacitance.[17]. The specific surface area capacitance of MCNTs is 111 μm cm^{-2}, which is much higher than that of commercial activated carbon (about 6 μm cm^{-2}). The result indicated a favorable balance between specific surface area and pore size distribution, further resulting in an enhanced capacitve behavior. Regone plots are also presented in Figure 3d. The energy density can be estimated to be 22.1 Wh kg^{-1} for MCNTs and 18.5 Wh kg^{-1} for CCNTs at a power density of 200 W kg^{-1}. More significantly, the energy density is still as high as 16.4 Wh kg^{-1} for MCNTs even at a high power density of 8000 W kg^{-1} while only 12.2 Wh kg^{-1} for CCNTs at a power density of 4000 W kg^{-1}. The present results have shown that the as-designed MCNTs are a very promising electrode material for high performance supercapacitors, especially for high-rate charge/discharge operations.

Moreover, the as-synthesized MCNTs are also an excellent catalyst supports. It is noted that polydopamine has substantial functional groups, which are also beneficial for growing and anchoring metal nanocrystals. Based on this feature, here, Pt/MCNTs are exploited to catalyze electro-oxidation of methanol in acid medium via an in situ synthesis route, which represents a promising alternative for fuel cells.[18] Figure 3a and b show that Pt nanocrystals with diameters of ~ 2-6 nm are homogeneously distributed onto the MCNTs frameworks. The statistical histogram of the particle diameter distribution was supplied in Figure S5. No free Pt nanocrystals can be observed. It is evident that Pt nanocrystals strongly absorb on the surface of MCNTs. The weight content of Pt in Pt/MCNTs catalyst is estimated to ~ 30% by the EDS analysis (See ESI).

The electro-oxidation performance of Pt/MCNTs was evaluated by cyclic volammetry (CV) and Chronoamperometry (CA) measurements. For comparison, the CCNTs were also used as catalyst supports to load Pt nanocrystals. The Pt/CCNTs and commercially E-TEK (30wt% Pt) catalysts have been studied under the same experimental conditions. Figure 3c shows the CV curves of Pt/MCNTs, Pt/CCNTs and E-TEK recorded at a scan rate of 20 mV s^{-1} in electrolytes of 1 M CH_3OH in 0.5 M H_2SO_4. It can be observed that the onsets of methanol oxidation peaks begin at 0.4 V vs. Ag/AgCl, and the peak potentials of methanol oxidation are similar, at about 0.68 V vs. Ag/AgCl in the forward scan. It is noted that the oxidation current observed with Pt/MCNTs is considerably higher than those of the Pt/CCNTs and E-TEK catalysts, showing a significant improvement in the catalytic activity. Very interestingly, for the Pt/MCNTs catalyst, the current density of the forward scan (I_f) is much higher than that of the backward scan (I_b). It is well known that the current density ratio (I_f/I_b) is a critical parameter to evacuate the tolerance of the catalyst to the accumulated intermediate carbonaceous species.[19] A higher ratio indicates more effective removal of the poisoning species on the catalyst surface. The I_f/I_b ratio of Pt/MCNTs is 1.29, close to that of Pt/CCNTs (1.25) and much higher than that of E-TEK (0.69), further confirming that Pt/MCNTs exhibits excellent catalytic efficiency and good

tolerance toward poisoning species for the electro-oxidation of methanol. The CA curves of Pt/MCNTs, Pt/CCNTs and E-TEK are shown in Figure 3d, which reflect the activity and stability of the catalyst to catalyze methanol. Under a given potential of 0.6 V, Pt/MCNTs shows a higher initial current and a slower decay of the peak current with the time, suggesting a better catalytic activity and stability than Pt/CCNTs and E-TEK.

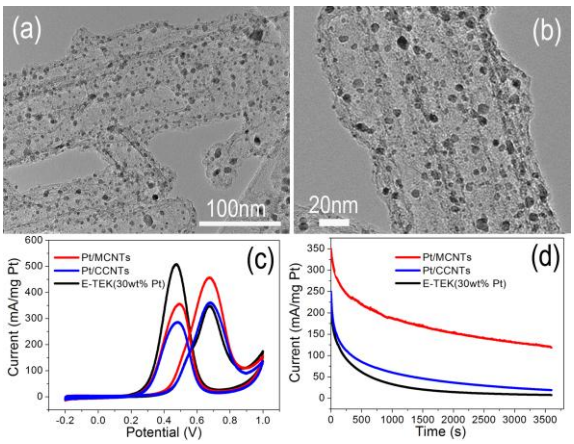

Fig. 3 (a) Low-magnification, (b) high-magnification TEM images of Pt nanoparticles supported on MCNTs. (c) CV curves recorded at 20 mV s^{-1} and (d) CA curves measured at 0.6 V of methanol electro-oxidation on the Pt/MCNTs, Pt/CCNTs and commercial E-TEK (30wt% Pt) catalyst at room temperature, respectively.

The Pt/MCNTs with high methanol catalytic activity are mainly attributed to the maximum utilization of Pt nanocrystals. This is because the mesoporous feature of support ensures the sufficient contact between Pt nanocrystals and the reactant. Furthermore, the well-distributed Pt nanocrystals with small size distribution on the MCNTs framework offer high-surface-area access to the active sites. On the other hand, Pt/polydopamine composites have firstly been synthesized by an integration of Pt and polydopmine with chemical bonds, which can firmly anchor the Pt nanocrystas on the surface of polydopamine. After carbonization, Pt nanocrystals are still well-dispersed on the surface of MCNTs, proving that Pt nanocrystals have been well anchored. Also, our strategy avoids the agglomeration of Pt nanocrystals during the electrochemical process, further leading to the improvement of catalytic stability and tolerance.

In conclusion, functional mesoporous carbon nanotubes (MCNTs) have been designed and successfully synthesized by a facile route for electrochemical energy storage. The MCNTs, when applied as supercapacitor electrode in 1 M H_2SO_4, demonstrate high specific capacitance (249 F g^{-1} at 0.5 A g^{-1}) and rate capability (~ 75% capacity retention at 20 A g^{-1}). More significantly, the as-synthesized MCNTs are also an excellent catalyst supports. The in situ synthesis of metal nanocrystals integrated with the MCNTs (Pt/MCNTs) has been developed for direct methanol fuel cells (DMFCs) applications, which demonstrated high methanol oxidation activity, good tolerance and stability. It is reckoned that the present study also shed light to the design of carbon and metal-carbon hybrid structures for other applications.

This work was supported by the National Natural Science Foundation of China (20925621, 20906027), the Special Projects for Key Laboratories in Shanghai (10DZ2211100), the Shanghai Shuguang Scholars Tracking Program (10SG31), the Basic Research Program of Shanghai (10JC1403300, 10JC1403600), the Shanghai Pujiang Program (09PJ1403200) and the Special Projects for Nanotechnology of Shanghai (1052nm02300).

Notes and references

[a] *Key Laboratory for Ultrafine Materials of Ministry of Education, School of Materials Science and Engineering, East China University of Science & Technology, Shanghai 200237, China. (Chunzhong Li). Fax: 86- 21- 6425- 0624; Tel: 86- 21- 6425- 0949; E-mail: czli@ecust.edu.cn*

[b] *Temasek Laboratories, Nanyang Technological University, Singapore 637553, Singapore. E-mail: asjma@ntu.edu.sg (Jan Ma)*

[c] *School of Materials Science and Engineering, Nanyang Technological University, Singapore 639798, Singapore*

† Electronic Supplementary Information (ESI) available: [details of any supplementary information available should be included here]. See DOI: 10.1039/b000000x/

1 (a) A. S. Arico, P. Bruce, B. Scrosati, J. –M. Tarascon and W. V. Schalkwijk, *Nat. Mater.*, 2005, **4**, 366; (b) M. Winter and R. J. Brodd, *Chem. Rev.*, 2004, **104**, 4245; (c) S. J. Guo and S. J. Dong, *Chem. Soc. Rev.*, 2011, **40**, 2644.

2 (a) L. L. Zhang and X. S. Zhao, *Chem. Soc. Rev.*, 2009, **38**, 2520; (b) R. H. Baughman, A. A. Zakhidov and W. A. Heer, *Science*, 2002, **297**, 787.

3 J. Liu, Z. Yue and H. Fong, *Small*, 2009, **5**, 536.

4 C. M. Niu, E. K. Sichel, R. Hoch, D. Moy and H. Tennent, *Appl. Phys. Lett.*, 1997, **70**, 1480.

5 H. Zhang, G. Cao, Y. Yang and Z. Gu, *J. Electrochem. Soc.*, **2008**, *155*, k19.

6 B. Hu, K. Wang, L. H. Wu, S. H. Yu, M. Antonietti and M. M. Titirici, *Adv. Mater.*, 2010, **22**, 813.

7 (a) P. Kundu, A. Halder, B. Viswanath, D. Kundu, G. Ramanath and N. Ravishankar, *J. Am. Chem. Soc.*, 2010, **132**, 20; (b) S. J. Guo, S. J. Dong and E. K. Wang, Adv. Mater., 2010, **22**, 1269.

8 (a) A. Bezryadin, C. N. Lau and M. Tinkham, *Nature*, 2000, **404**, 971; (b) B. M. Quinn, C. Dekker and S. G. Lemay, *J. Am. Chem. Soc.*, 2005, **127**, 6146.

9 H. Jiang, L. P. Yang, C. Z. Li, C. Y. Yan, P. S. Lee, and J. Ma, *Energy Environ. Sci.*, 2011, **4**, 1813.

10 (a) H. Pan, C. K. Poh, Y. P. Feng and J. Y. Lin, *Chem. Mater.*, 2007, **19**, 6120; (b) J. S. Ye, X. Liu, H. F. Cui, W. D. Zhang, F. S. Sheu and T. M. Lim, *Electrochem. Commun.*, 2005, **7**, 249.

11 E. Raymundo-Piñero, F. Leroux and F. Béguin, *Adv. Mater.*, 2006, **18**, 1877.

12 D. N. Futaba, K. Hata, T. Yamada, T. Hiraoka, Y. Hayamizu, Y. Kakudate, O. Tanaike, H. Hatori, M. Yumura and S. Iijima, *Nat. Mater.* 2006, **5**, 987.

13 J. Yan, T. Wei, B. Shao, F. Q. Ma, Z. J. Fan, M. L. Zhang, C. Zheng, Y. C. Shang, W. Z. Qian and F. Wei, *Carbon*, 2010, **48**, 1731.

14 Y. X. Xu, K. X. Sheng, C. Li andG. Q. Shi, *ACS Nano*, 2010, **4**, 4324.

15 E. Raymundo-Piñero, K. Kierzek, J. Machnikowski and F. Béguin, *Carbon*, 2006, **44**, 2498.

16 Z. Chen, Y. C. Qin, D. Weng, Q. F. Xiao, Y. T. Peng, X. L. Wang, H. X. Li, F. Wei and Y. F. Lu, *Adv. Func. Mater.*, 2009, **19**, 3420.

17 (a) D. Hulicova-Jurcakova, M. Kodama, S. Shiraishi, H. Haori, Z. H. Zhu and G. Q. Lu, *Adv. Funct. Mater.*, 2009, **19**, 1800; (b) L. Zhao, L. Z. Fan, M. Q. Zhou, H. Guan, S. Y. Qiao, M. Antonietti and M. M. Titirici, *Adv. Mater.*, 2010, **22**, 5202.

18 Y. Zhao, L. Z. Fan, H. Z. Zhong, Y. F. Li and S. H. Yang, *Adv. Funct. Mater.*, 2007, **17**, 1537.

19 Y. Y. Liang, M. G. Schwab, L. J. Zhi, E. Mugnaioli, U. Kolb, X. L. Feng and K. Müllen, *J. Am. Chem. Soc.* 2010, **132**, 15030.

(For Table of Content use only)

Table of Content Image

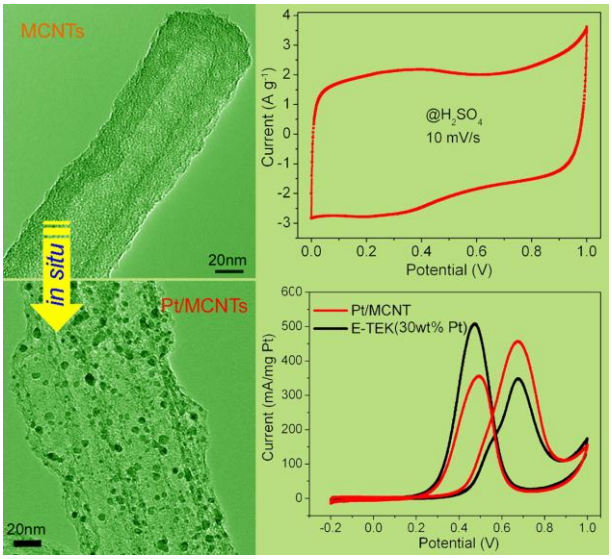
MCNTs
20nm
in situ
Pt/MCNTs
20nm
Current (A g-1)
@H2SO4
10 mV/s
Potential (V)
Pt/MCNT
E-TEK(30wt% Pt)
Current (mA/mg Pt)
Potential (V)